

## N O T I C E

THIS DOCUMENT HAS BEEN REPRODUCED FROM  
MICROFICHE. ALTHOUGH IT IS RECOGNIZED THAT  
CERTAIN PORTIONS ARE ILLEGIBLE, IT IS BEING RELEASED  
IN THE INTEREST OF MAKING AVAILABLE AS MUCH  
INFORMATION AS POSSIBLE

DOE/NASA/2593-79/10  
NASA TM-79296

(NASA-TM-79296) AN ANALYTICAL STUDY OF  
NITROGEN OXIDES AND CARBON MONOXIDE  
EMISSIONS IN HYDROCARBON COMBUSTION WITH  
ADDED NITROGEN, PRELIMINARY RESULTS (NASA)  
17 p HC A02/MF A01

N80-13721

Unclas  
46299

CSCL 13B G3/45

# **AN ANALYTICAL STUDY OF NITROGEN OXIDES AND CARBON MONOXIDE EMISSIONS IN HYDROCARBON COMBUSTION WITH ADDED NITROGEN — PRELIMINARY RESULTS**

David A. Bittker  
National Aeronautics and Space Administration  
Lewis Research Center

Work performed for  
**U.S. DEPARTMENT OF ENERGY**  
**Energy Technology**  
**Fossil Fuel Utilization Division**

Prepared for  
Twenty-fifth International Gas Turbine Conference  
sponsored by the American Society of Mechanical Engineers  
New Orleans, Louisiana, March 9-13, 1980

AN ANALYTICAL STUDY OF NITROGEN OXIDES AND CARBON MONOXIDE

EMISSIONS IN HYDROCARBON COMBUSTION WITH ADDED

NITROGEN - PRELIMINARY RESULTS

by David A. Bittker

National Aeronautics and Space Administration  
Lewis Research Center  
Cleveland, Ohio

INTRODUCTION

One of the major efforts in the development of gas turbines for ground power generation is their adaptation to the use of coal-derived liquid fuels. The wide range of properties of these synthetic liquid fuels leads to many problems. A recent summary of coal derived liquid fuel properties and their potential problems in turbine combustion is given in Ref. 1. The present paper focuses on the problem of increased emissions. The main question is how much the oxides of nitrogen ( $\text{NO}_x$ ) emissions will be increased by the increased amount of organic nitrogen compounds contained in these synthetic liquids. Another question is whether this fuel-bound nitrogen (FBN) will have any significant effect upon the carbon monoxide (CO) emissions from synthetic fuel combustion.

The present work was undertaken to investigate these questions as one part of the Critical Research and Technology program funded by the Department of Energy at the Lewis Research Center. The primary purpose of this work is to analytically determine the effect of combustion operating conditions on the conversion of FBN to  $\text{NO}_x$ . The effect of FBN and of operating conditions on CO emissions was also examined. Propane-air was chosen as the combustible mixture for the first series of computations. The combustor model was assumed to be a two-stage, adiabatic, perfectly-stirred reactor. Chemical modeling of the oxidation of propane and the formation of  $\text{NO}_x$  was done using a fifty-seven reaction mechanism. The use of two-stage combustion to minimize  $\text{NO}_x$  formation has been reported by several investigators (2 to 4).<sup>1</sup> The greatest  $\text{NO}_x$

<sup>1</sup>Numbers in parentheses designate references at end of paper.

reduction is achieved by burning with a rich primary mixture and then diluting with air for quite lean second-stage combustion.

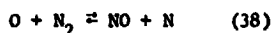
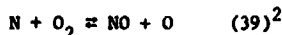
A wide range of operating conditions was used for these computations. Primary equivalence ratio,  $\Phi_p$ , was varied from 0.5 to 1.7. Dilution air was added in the secondary zone, as necessary, to give a secondary equivalence ratio,  $\Phi_s$ , of either 0.5 or 0.7. Primary stage residence time varied from approximately 12 to 20 msec and secondary stage residence times of approximately 1, 2, and 3 msec were used. Three different amounts of FBN were used in the computations, namely 0.5, 1.0, and 2.0 percent by weight of the initial fuel. All computations were performed for a constant pressure of 5 atm and initial mixture temperatures ranged from 608 to 650 K.

Computations were performed using the NASA Lewis General Chemical Kinetics Program (5), which was modified to perform stirred-reactor model computations. The nonlinear algebraic equations given in Refs. 6 and 7 for multicomponent, chemically rate-limited homogeneous reaction in a perfectly-stirred reactor were used. Solution of these equations by the modified Newton-Raphson iteration procedure given in Ref. 6 was programmed and incorporated as a subroutine into the general chemical kinetics program.

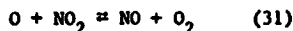
Results are presented for  $\text{NO}_x$  and CO concentrations as a function of  $\Phi_p$ ,  $\Phi_s$  and both primary and secondary residence times, as well as the amount of FBN. A limited comparison of the computed results with experimental results obtained under another task in the Critical Research and Technology program is also given. The comparison will show the good semi-quantitative agreement between our theoretical model and the experimental results. It should be mentioned that neither the theoretical computations nor the experimental work were meant to model a practical turbine combustor.

Moreover, the effects of initial temperature and pressure variation were considered of secondary importance. These conditions were not changed in either the experimental or the theoretical work.

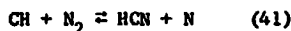
The chemistry of nitrogen oxide formation during combustion has been studied extensively for many years. Two good reviews of this topic are given in Refs. 8 and 9. In this paper we shall define nitrogen oxides or  $\text{NO}_x$  as the sum of nitric oxide (NO) and nitrogen dioxide ( $\text{NO}_2$ ) concentrations. Although the mechanism of  $\text{NO}_x$  formation in lean hydrocarbon combustion is fairly well known, our knowledge is still lacking for very rich mixtures (i.e., equivalence ratios from about 1.2 to 2). For lean combustion  $\text{NO}_x$  formation is explained mainly by the extended Zeldovich mechanism



and the additional reaction:



To explain experimental  $\text{NO}_x$  concentrations higher than computed values for rich mixtures Fenimore (10) suggested the direct reaction of hydrocarbon fragments with molecular nitrogen:



Both products of this reaction can lead to additional NO formation. The additional reactions of HCN, CN, and  $\text{NH}_i$  species are the unknowns in the path of complete understanding of  $\text{NO}_x$  formation. Jachimowski (11) showed that the addition of only reaction (41) to the fairly well known methane oxidation mechanism improved rich combustion NO prediction considerably. And more recently, Wakelyn, Jachimowski and Wilson (12) developed a comprehensive propane-air combustion mechanism. It employs not only reaction (41) but those involving HCN, CN, NCO, and NH species. When applied to computing NO concentrations for stirred-reactor combustion of rich propane-air mixtures (up to  $\Phi = 1.4$ ), this mechanism gave excellent agreement with experimental results obtained in their laboratory. These investigators also applied the stirred-reactor model and their propane-air chemical model in computations attempting to match experimental flame-tube emission data of Anderson (13). The computed and experimental results agreed quite satisfactorily.

In choosing the mechanism for the present computations we have, therefore, used a modification of the mechanism developed in Ref. 12. One of the key contributions of that work is the fact that the computed NO concentration is very sensitive to the rate constant,  $k_{41}$  for reaction (41). The authors used this fact to derive a new value for  $k_{41}$  which gave the best agreement between their computed and experimental results and this improved value of  $k_{41}$  was used in the present computations. The complete mechanism used in the present computations is given in Table I, along with rate constants and their sources. The first 40 reactions plus reaction 52 were sufficient for computations at  $\Phi_p$  values from 0.5 to 1.0. The full mechanism was used for all  $\Phi_p$  values greater than 1.0.

<sup>2</sup>Reactions are numbered to correspond to numbers in Table I.

In previous analytical modeling of fuel-bound nitrogen conversion to  $\text{NO}_x$  (4 and 13) the FBN has been simulated by simple species such as N, NH,  $\text{NH}_3$ , HCN, CN. This is necessary because of the complexity of the organic nitrogen compounds in synthetic fuels and the lack of detailed kinetic data on the pyrolysis of these compounds. The rationale for using one of these "model compounds" to represent FBN is detailed in Ref. 14. The basic assumption is that one of these simple species represents the major pyrolysis product of the more complicated molecule that can react to form  $\text{NO}_x$ . The work of Ref. 14 showed that computed results for NO conversion using N, NH, CN, and HCN are semiquantitatively similar. Inasmuch as our combustor model is quite idealized, we chose the simplest species, nitrogen atom, as our model compound for the FBN. It should be mentioned that using N as the model compound gives about 25 percent less conversion to  $\text{NO}_x$  than using the other model compounds. This is due to the importance of the reverse of reaction 38,  $\text{NO} + \text{N} \rightarrow \text{O} + \text{N}_2$ .

## RESULTS AND DISCUSSION

### Effect of Fuel-Bound Nitrogen

The main interest in this paper is the effect of FBN on both  $\text{NO}_x$  and CO final concentration. This effect is shown in Fig. 1 for  $\text{NO}_x$  and Fig. 2 for CO. In each figure computed final pollutant concentration, with no further dilution, is plotted against initial equivalence ratio,  $\Phi_p$ , from 0.5 to 1.7 for several different FBN contents. For these computations primary reaction volume was constant at  $4360 \text{ cm}^3$ , the shortest primary-zone residence time; secondary residence time was fixed at nominally 1 msec. These conditions were chosen to correspond to those used in the experimental flame tube work which will be described briefly in a following section. Secondary air was added when necessary to give a  $\Phi_g$  value of 0.7. Primary mixtures leaner than  $\Phi_p = 0.7$  were not diluted. It is observed in Fig. 1 that the minimum  $\text{NO}_x$  concentration is always obtained at a  $\Phi_p$  value between 1.4 and 1.5 for the range of  $\Phi_p$  shown. At the  $\Phi_p$  value for this minimum  $\text{NO}_x$  concentration the CO concentration (Fig. 2) always attains its maximum value. Although  $\text{NO}_x$  always increases as FBN is increased, the highest percent conversion of FBN to  $\text{NO}_x$  occurs for 0.5 percent FBN at the rich  $\Phi_p$  values. For example, at  $\Phi_p = 1.4$  the FBN conversions are approximately 25, 19, and 15 percent for initial FBN contents of 0.5, 1.0, and 2.0 percent, respectively. The decrease in FBN conversion with increased FBN content has been observed by others (14). The effect of FBN on CO formation is quite different. Figure 2 shows that any FBN decreases the final CO concentration. For  $\Phi_p = 1.4$ , the point of greatest CO concentration, any amount of FBN decreases the CO concentration by about 17 percent.

The effect of added FBN on final  $\text{NO}_x$  concentration can be seen better in Fig. 3 where the  $\text{NO}_x$  concentration is plotted against percent of FBN for several different primary equivalence ratios. This plot shows that the greatest percentage increase of  $\text{NO}_x$  concentration with added FBN occurs at the extremely lean and the very rich primary equivalence ratios. The absolute increase in  $\text{NO}_x$  concentration for a fixed addition of FBN does not change greatly with primary equivalence ratio. For example we can compare  $\text{NO}_x$  concentrations for 0 and for 0.5 percent FBN in the following table

$\Phi_p$	NO <sub>x</sub> concentration, ppm		Absolute change, ppm	Percent change
	0% FBN	0.5% FBN		
0.6	155	500	345	222
.9	2130	2400	270	13
1.4	110	340	230	209

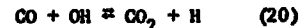
The absolute changes in NO<sub>x</sub> concentration are between 230 and 345 ppm. But this translates to a change of about 200 percent at the highest and lowest  $\Phi_p$  values and a change of only 13 percent at  $\Phi_p = 0.9$ , where NO<sub>x</sub> formation is highest without FBN present. Also in Fig. 3, the decrease in NO<sub>x</sub> concentration gradient as percent FBN rises above 0.5 is particularly noticeable at  $\Phi_p = 1.4$ , the condition for minimum NO<sub>x</sub> formation in general.

#### Effect of Secondary Dilution

The effect of additional dilution was studied by repeating the second stage computations for a  $\Phi_s$  value of 0.5 instead of 0.7. The results for final NO<sub>x</sub> concentration are shown in Fig. 4 and for CO concentration in Fig. 5. All other conditions are the same as in Figs. 1 and 2. Final pollutant concentration is again plotted against  $\Phi_p$  for various amounts of FBN. Comparison of Figs. 4 and 1 and Figs. 5 and 2 show that the trends are very much the same. However, both pollutant concentration levels have been significantly reduced by the added dilution. For a better quantitative comparison of dilution effects we have replotted the 1 percent FBN NO<sub>x</sub> formation curves from Figs. 1 and 4 together in Fig. 6(a). Likewise the 1 percent FBN CO formation curves from Figs. 2 and 5 are replotted together in Fig. 6(b). From these plots it is seen that the greatest percentage reduction due to additional dilution in both NO<sub>x</sub> and CO is at a  $\Phi_p$  value close to 1.4, the value for minimum NO<sub>x</sub>. NO<sub>x</sub> is reduced by about 47 percent and CO by 57 percent due to the additional dilution.

The observed concentration reductions are, of course, the combined effect of physical dilution of the primary gas and the chemical reaction in the secondary-stage combustion. It is of interest to compare these two effects for the present model and this can be done with the help of Table II. In this table we have listed three different values of NO<sub>x</sub> and CO concentration for several  $\Phi_p$  values and for secondary dilution to both  $\Phi_s = 0.7$  and  $\Phi_s = 0.5$ . In addition to the secondary exhaust gas concentration we have listed the primary exhaust gas concentration and also the diluted primary exhaust gas concentration before the secondary chemical reaction. For NO<sub>x</sub> the table shows that only the dilution of the primary mixture determines final concentration for the lean and stoichiometric  $\Phi_p$  values of 0.8 and 1.0. For both secondary dilutions the NO<sub>x</sub> concentration is increased by at most 2 percent during the secondary reaction. For example, at  $\Phi_p = 1.0$  and  $\Phi_s = 0.7$  NO<sub>x</sub> concentration increases from 2242 to 2291 ppm during the secondary reaction. For the rich primary mixtures, however, there is significant chemical reaction forming NO<sub>x</sub> in the secondary stage when dilution is to  $\Phi_s = 0.7$ . At  $\Phi_p = 1.4$ , for example, the secondary chemical reaction increases NO<sub>x</sub> by 37 percent from 327 to 447 ppm. For dilution to  $\Phi_s = 0.5$  there is, however, negligible chemical reaction forming NO<sub>x</sub> when  $\Phi_p$  is 1.2 and 1.4. The probable reason for this can be seen in Fig. 7, where secondary reaction temperature is plotted as a function of  $\Phi_p$  for both secondary dilutions. The same 1.0 percent FBN content as in Figs. 6(a) and (b) was used. The reaction tem-

perature is reduced by more than 300 K for all  $\Phi_p$  values from 0.8 to 1.7 when  $\Phi_s$  goes from 0.7 to 0.5. This drop in temperature could easily quench the NO<sub>x</sub> formation reactions which are very temperature dependent. The situation is quite different for CO. Table II shows that the final CO concentration is determined mainly by secondary stage chemical reaction for all conditions. This is especially true for the rich primary mixtures in which CO concentration is very high. The reason for the quite different behavior of CO concentration is the lack of temperature dependence of the main CO oxidation reaction



A drop of 300 K in temperature, as shown in Fig. 7, has a negligible effect on the rate constant of this reaction.

#### Effect of Primary and Secondary Residence Times

Primary zone residence time was increased by changing the reaction volume by factors of 1.2 and 1.4. Thus a typical residence time of 12 msec at the smallest reaction volume was changed to about 17 msec for the largest volume. No significant effect or primary residence time was predicted for either pollutant. Typical examples of the variation of NO<sub>x</sub> and CO with primary residence time are shown in Figs. 8 and 9. Pollutant concentration is plotted against primary equivalence ratio for mixtures containing 1.0 percent fuel-bound nitrogen using three different primary residence times.

All secondary-stage computations were performed using three different reaction volumes. They were chosen to give nominal secondary residence time values of 1, 2, and 3 msec. Typical plots of NO<sub>x</sub> concentration versus secondary residence time with  $\Phi_p$  as a parameter are shown in Figs. 10(a) and (b). For Fig. 10(a) the secondary stage  $\Phi_s$  value is 0.7 and for Fig. 10(b) it is 0.5. Mixtures containing one percent FBN were used for the computations. For dilution to  $\Phi_s = 0.7$ , we see that the NO<sub>x</sub> results are somewhat sensitive to residence time variation for the very rich mixtures ( $\Phi_p = 1.4$  and 1.7). There is a 35 percent increase in NO<sub>x</sub> concentration as residence time increases from 1 to 3 msec at  $\Phi_p = 1.4$ . When the secondary dilution is to  $\Phi_s = 0.5$ , however, Fig. 10(b) shows that final NO<sub>x</sub> concentration is completely independent of secondary residence time. These results are explained by the temperature effect on NO<sub>x</sub> forming reactions just discussed. There can only be an effect of secondary residence time on NO<sub>x</sub> concentration where there is chemical reaction in the secondary zone. It has just been shown that NO<sub>x</sub> concentration increases in the secondary zone only for rich mixtures diluted to  $\Phi_s = 0.7$ . The effect of secondary residence time on CO concentration is shown in Figs. 11(a) and (b). The plots are exactly analogous to Figs. 10(a) and (b). In contrast to NO<sub>x</sub>, the CO concentration decreases as residence time increases for all values of  $\Phi_p$  and both secondary dilutions. Moreover, the rate of decrease of CO concentration with residence time is fairly independent of both primary equivalence ratio and amount of secondary dilution. The trends shown here, for 1.0 percent FBN in the fuel, are similar to those for other added amounts of FBN. When no added FBN is present, the trends are the same especially for secondary dilution to  $\Phi_s = 0.5$ . The only difference is observed for  $\Phi_s = 0.7$ . For this dilution the NO<sub>x</sub> concentration increases more sharply with increasing secondary residence time for  $\Phi_p = 1.4$  and 1.7 than shown in Fig. 10(a).

### Comparison with Experimental Data

Experimental emission measurements are being made by G. Wolfbrandt and D. Schultz at the Lewis Research Center in another part of the CRT program. Their apparatus is a two-stage flame tube. A highly turbulent hydrocarbon-air mixture is burned in two stages, with dilution in the second stage exactly as described for the present idealized stirred-reactor model. Both propane-air and propane-toluene-air mixtures are being used in this program and pyridine is added to simulate fuel bound nitrogen. The purpose of this experimental work is the same as for the present theoretical study; that is, to determine the effect of operating conditions on FBN conversion to  $\text{NO}_x$ . To test whether the idealized stirred-reactor model predicts the qualitative experimental trends we have made plots comparing experimental and computed results. Figure 12 shows experimental and computed  $\text{NO}_x$  concentration vs.  $\Phi_p$  and Fig. 13 shows CO concentration vs.  $\Phi_p$ . These results are for propane-air with no added FBN. The experimental points are the first data from the flame-tube experiment. For both pollutants the qualitative agreement can be seen to be quite good. Moreover, the quantitative agreement steadily improves as we go to rich primary equivalence ratios. For this latter region agreement is within  $\pm 50$  percent.

Some possible sources of discrepancy are: (1) an incomplete chemical model of the combustion; (2) experimental heat losses; and (3) mixing nonhomogeneity during the experiment.

The present chemical model should be equivalent to the model of Ref. 12 in matching the data of Anderson (13). We find this to be true when we compare the results of our primary zone computations with the experimental results of Anderson. Our computed primary zone  $\text{NO}_x$  and CO concentrations are in good agreement with Anderson's results for all equivalence ratios. Therefore the observed discrepancies between computed and experimental second-stage pollutant concentrations are probably due to mixing nonhomogeneity and heat losses in the second stage combustion. One important point is the fact that there is a finite length of mixing and chemical reaction at the entrance to the secondary zone for the experiment. The computational model assumes instantaneous mixing of the dilution air with the primary exhaust gases before the secondary reaction begins. Apparently the experimental effects are less important when the primary-zone burning is rich.

### SUMMARY OF RESULTS

In this study we have predicted analytically the effect of operating conditions on pollutant formation in two-stage combustion. In particular we have studied the effect of these conditions on fuel bound nitrogen conversion to  $\text{NO}_x$  and also on CO formation. Propane-air mixtures were assumed to burn in a two-stage, adiabatic, perfectly-stirred reactor. Various amounts of fuel-bound nitrogen, up to 2 percent by weight as nitrogen atoms, were used. The product gases of the primary stage were diluted by added air in the second stage to an overall equivalence ratio of either 0.7 or 0.5. The computed results were compared with a limited amount of experimental data. The important results of this work may be summarized as follows:

1. Minimum  $\text{NO}_x$  formation occurs in general when the primary zone equivalence ratio is between 1.4 and 1.5. However, for this range of values, the CO formation is at its highest level.

2. The percentage conversion of fuel bound nitrogen to  $\text{NO}_x$  is greatest for small percentages of FBN and decreases as FBN content is raised above 0.5 percent by weight.

3. The final concentrations of  $\text{NO}_x$  and CO are significantly reduced by additional secondary dilution from  $\Phi_s = 0.7$  to  $\Phi_s = 0.5$ . The extra dilution lowers the secondary reaction temperature by about 300 K and thus suppresses all secondary-stage  $\text{NO}_x$  reactions. Therefore, the change in  $\text{NO}_x$  concentration due to the added dilution is strictly an effect of more dilution to the primary mixture. For CO, however, the final CO concentration is always a combined result of diluting the primary mixture and secondary-zone chemical reaction. This is because temperature has very little effect on CO destruction chemistry in the present model.

4. For secondary dilution to  $\Phi_s = 0.5$ ,  $\text{NO}_x$  concentration is completely independent of secondary residence time. This is because of the suppression of  $\text{NO}_x$  reactions due to the low secondary zone reaction temperatures. For secondary dilution of rich primary mixtures to  $\Phi_s = 0.7$ ,  $\text{NO}_x$  forms in the secondary zone due to chemical reaction. Therefore  $\text{NO}_x$  concentration increases with increasing secondary residence time for these rich primary mixtures only. Only in this region is chemical reaction important in the secondary zone. The final CO concentration always decreases with increasing secondary residence time because, in the present model, chemical reaction to destroy CO is not strongly affected by temperature.

5. Final  $\text{NO}_x$  and CO concentrations show negligible dependence on primary zone residence time.

6. Comparison of computed results with limited experimental data indicates that there is good agreement in trends between the idealized theoretical model and the experiment. The quantitative agreement steadily improves as the primary equivalence ratio increases. For the values of greatest interest ( $\Phi_p \geq 1.4$ ) the agreement between theory and experiment is within  $\pm 50$  percent. Apparently, effects of experimental heat transfer losses and mixing nonhomogeneity are less for these rich primary mixtures. These last two factors were not considered in the theoretical combustion model.

### CONCLUDING REMARKS

This theoretical study reinforces the well-known idea that emissions of  $\text{NO}_x$  and CO can be reduced by two-stage combustion, burning rich in the primary zone and lean in the secondary. Our computations indicate that modest additional secondary dilution, from equivalence ratio 0.7 to 0.5, has a strong effect in reducing the absolute level of  $\text{NO}_x$  and CO concentrations. Also it was found that there is a large increase in  $\text{NO}_x$  formation due to a small amount (0.5 percent) of added FBN in the fuel. Our computed emission concentrations do not have a direct correlation with actual combustor emissions. However, the trends do indicate that removing only a moderate amount of the FBN from a real fuel during refining may not be sufficient to meet government emission standards.

Future synthetic fuels contain higher amounts of olefins and aromatic hydrocarbons than current petroleum fuels. The lower hydrogen/carbon ratio of the synthetic fuels will also affect pollutant formation. Therefore, we hope to perform additional computations using as the fuel a mixture of toluene ( $\text{C}_7\text{H}_8$ ) and propane. The results for  $\text{NO}_x$  and CO emissions can then be compared with experimental flame tube results using the same fuel mixture.

#### ACKNOWLEDGEMENT

I wish to express my appreciation to Gary Wolfbrandt and Don Schultz for allowing me to publish some of their experimental data.

#### REFERENCES

- 1 Pillsbury, P. W., et. al., "Investigative Combustion Turbine Burner Performance with Coal Derived Liquids Having High Fuel-Bound Nitrogen," ASME Paper No. 78-GT-126, Apr. 1978.
- 2 Yamagishi, K., et. al., "A Study of  $\text{NO}_x$  Emission Characteristics in Two-Stage Combustion," International Symposium on Combustion, 15th, Combustion Institute, Pittsburgh, Pa., 1975, pp. 1157-1166.
- 3 Martin, F. J. and Dederick, P. K., " $\text{NO}_x$  From Fuel Nitrogen in Two-Stage Combustion," International Symposium on Combustion, 16th, Combustion Institute, Pittsburgh, Pa., 1977, pp. 191-198.
- 4 Takagi, T., Tatsumi, T., and Ogasawara, M., "Nitric Oxide Formation from Fuel Nitrogen in Staged Combustion: Roles of HCN and  $\text{NH}_3$ ," Combustion and Flame, Vol. 35, No. 1, May 1979, pp. 17-25.
- 5 Bittker, D. A. and Scullin, V. J., "General Chemical Kinetics Computer Program for Static and Flow Reactions, with Application to Combustion and Shock-Tube Kinetics," NASA TN D-6586, 1972.
- 6 Pratt, D. T., "FSR: A Computer Program for Calculation of Steady-Flow Homogeneous Combustion Reaction Kinetics," WSU-Bull.-336, Washington State University, Pullman, Wash., 1974.
- 7 Jones, A. and Prothero, A., "The Solution of the Steady-State Equations for an Adiabatic Stirred Reactor," Combustion and Flame, Vol. 12, Oct. 1968, pp. 457-464.
- 8 Bowman, C. T., "Kinetics of Pollutant Formation and Destruction in Combustion," Progress in Energy and Combustion Science, Vol. 1, No. 1, 1975, pp. 33-45.
- 9 Haynes, B. S., "Kinetics of Nitric Oxide Formation in Combustion," Alternative Hydrocarbon Fuels: Combustion Kinetics, C. T. Bowman and J. Birkeland, eds., American Institute of Aeronautics and Astronautics, New York, 1978, pp. 359-394.
- 10 Fenimore, C. P., "Formation of Nitric Oxide in Premixed Hydrocarbon Flames," International Symposium on Combustion, 13th, Combustion Institute, Pittsburgh, Pa., 1971, pp. 373-380.
- 11 Jachimowski, C. J., "Analytical Study of Mechanisms for Nitric Oxide Formation During Combustion of Methane in a Jet-Stirred Combustor," NASA TN D-8098, 1975.
- 12 Wakelyn, N. T., Jachimowski, C. J., and Wilson, C. H., "Experimental and Analytical Study of Nitric Oxide Formation During Combustion of Propane in a Jet-Stirred Combustor," NASA TP-1181, 1978.
- 13 Anderson, D. N., "Effect of Premixing on Nitric Oxide Formation," NASA TM X-68220, 1973.
- 14 Caretto, L. S., "Modeling the Gas Phase Kinetics of Fuel Nitrogen," W88-CI Paper 76-12, Apr. 1976.
- 15 Olson, D. B. and Gardiner, W. C., "Combustion of Methane in Fuel-Rich Mixtures," Combustion and Flame, Vol. 32, No. 2, June 1978, pp. 151-161.
- 16 Wilson, W. E., Jr., "A Critical Review of the Gas Phase Reaction Kinetics of the Hydroxyl Radical," Journal of Physical and Chemical Reference Data, Vol. 1, No. 2, 1972, pp. 535-573.
- 17 Baulch, D. L., et. al., Evaluated Kinetic Data for High Temperature Reactions, Vol. 1: Homogeneous Gas Phase Reactions of the H<sub>2</sub>-O<sub>2</sub> System, CRC Press, Cleveland, O., 1972.
- 18 Hampson, R. F., Jr. and Garvin, D., eds., "Reaction Rate and Photochemical Data for Atmospheric Chemistry, 1977," NBS-SP-513, National Bureau of Standards, Washington, D.C., May 1978.
- 19 Schofield, K., "An Evaluation of Kinetic Rate Data for Reactions of Neutrals of Atmospheric Interest," Planetary and Space Science, Vol. 15, 1967, pp. 643-670.

TABLE I. REACTION MECHANISM FOR PROPANE-AIR COMBUSTION

Reaction number	Reaction	Rate constant <sup>a,b</sup>			Reference
		A	n	θ	
1	$M + C_3H_8 \rightleftharpoons C_2H_5 + CH_3 + M$	$5.0 \times 10^{15}$	0.0	32 713	12
2	$C_2H_5 \rightleftharpoons C_2H_4 + H$	$3.16 \times 10^{13}$		20 483	12
3	$O + C_2H_6 \rightleftharpoons CH_3 + HCO$	$2.26 \times 10^{13}$		1 359	12
4	$O + C_2H_6 \rightleftharpoons CH_2O + CH_2$	$2.5 \times 10^{13}$		2 516	12
5	$CH_2 + O_2 \rightleftharpoons HCO + OH$	$1.0 \times 10^{14}$		1 862	12
6	$CH_3 + C_3H_8 \rightleftharpoons CH_4 + C_3H_7$	$2.0 \times 10^{13}$		5 184	12
7	$M + CH_4 \rightleftharpoons CH_3 + H + M$	$6.7 \times 10^{17}$		46 900	15
8	$H + CH_4 \rightleftharpoons CH_3 + H_2$	$1.26 \times 10^{14}$		5 989	12
9	$O + CH_4 \rightleftharpoons CH_3 + OH$	$2.0 \times 10^{13}$		4 640	12
10	$OH + CH_4 \rightleftharpoons CH_3 + H_2O$	$3.0 \times 10^{13}$		3 020	12
11	$CH_3 + O_2 \rightleftharpoons CH_2O + OH$	$7.0 \times 10^{11}$		4 530	15
12	$CH_3 + O \rightleftharpoons CH_2O + H$	$6.8 \times 10^{13}$		0.0	15
13	$CH_2O + H \rightleftharpoons HCO + H_2$	$2.0 \times 10^{13}$		1 660	15
14	$CH_2O + O \rightleftharpoons HCO + OH$	$5.0 \times 10^{13}$		2 300	15
15	$CH_2O + OH \rightleftharpoons HCO + H_2O$	$5.0 \times 10^{15}$		6 540	15
16	$HCO + O \rightleftharpoons CO + OH$	$3.0 \times 10^{13}$		0.0	15
17	$HCO + H \rightleftharpoons CO + H_2$	$2.0 \times 10^{13}$		0.0	15
18	$HCO + OH \rightleftharpoons CO + H_2O$	$3.0 \times 10^{11}$		0.0	15
19	$M + HCO \rightleftharpoons H + CO + M$	$3.0 \times 10^{14}$		7 400	15
20	$CO + OH \rightleftharpoons CO_2 + H$	$3.1 \times 10^{11}$		300	16
21	$M + CO + O \rightleftharpoons CO_2 + M$	$2.8 \times 10^{13}$		-2 285	15
22	$CO + O_2 \rightleftharpoons CO_2 + O$	$1.2 \times 10^{11}$		17 615	15
23	$H + O_2 \rightleftharpoons OH + O$	$2.2 \times 10^{16}$		8 450	17
24	$O + H_2 \rightleftharpoons OH + H$	$1.8 \times 10^{10}$	1.0	4 480	
25	$H_2 + OH \rightleftharpoons H_2O + H$	$5.2 \times 10^{13}$	.0	3 270	15
26	$O + H_2O \rightleftharpoons 2 OH$	$6.8 \times 10^{13}$	.0	9 240	17
27	$H + O_2 + M \rightleftharpoons HO_2 + M$	$2.43 \times 10^{15}$	.0	-290	18
28	$M + O_2 \rightleftharpoons 2 O + M$	$1.9 \times 10^{11}$	.5	48 160	15
29	$M + H_2 \rightleftharpoons 2 H + M$	$2.2 \times 10^{12}$	.5	46 600	15
30	$H + OH + M \rightleftharpoons H_2O + M$	$7.6 \times 10^{23}$	-2.6	0.0	15
31	$H + CH_3 \rightleftharpoons H_2 + CH_2$	$2.7 \times 10^{11}$	.67	12 934	12
32	$O + CH_3 \rightleftharpoons OH + CH_2$	$1.9 \times 10^{11}$	.68	12 934	12
33	$OH + CH_3 \rightleftharpoons H_2O + CH_2$	$2.7 \times 10^{11}$	.67	12 934	12
34	$HO_2 + NO \rightleftharpoons NO_2 + OH$	$2.0 \times 10^{13}$	0.0	1 200	18
35	$O + NO_2 \rightleftharpoons NO + O_2$	$1.0 \times 10^{13}$		300	18
36	$NO + O + M \rightleftharpoons NO_2 + M$	$9.4 \times 10^{14}$		-970	18
37	$NO_2 + H \rightleftharpoons NO + OH$	$7.2 \times 10^{14}$		970	19
38	$O + N_2 \rightleftharpoons NO + N$	$7.8 \times 10^{13}$		38 000	18
39	$N + O_2 \rightleftharpoons NO + O$	$6.4 \times 10^9$	1.0	3 145	12
40	$N + OH \rightleftharpoons NO + H$	$4.0 \times 10^{13}$	.0	0.0	12
41	$CH + N_2 \rightleftharpoons HCN + N$	$1.5 \times 10^{11}$	.0	9 562	12
42	$CN + H_2 \rightleftharpoons HCN + H$	$6.0 \times 10^{13}$	.0	2 669	12
43	$O + HCN \rightleftharpoons OH + CN$	$1.4 \times 10^{11}$	.68	8 506	12
44	$OH + HCN \rightleftharpoons CH + H_2O$	$2.0 \times 10^{11}$	.60	2 516	12
45	$CN + O_2 \rightleftharpoons NCO + O$	$3.2 \times 10^{13}$	.0	505	12
46	$CN + CO_2 \rightleftharpoons NCO + CO$	$3.7 \times 10^{12}$	.0	0.0	12
47	$H + NCO \rightleftharpoons NH + CO$	$2.0 \times 10^{13}$	.0	0.0	12
48	$NH + OH \rightleftharpoons N + H_2O$	$5.0 \times 10^{11}$	.5	1 006	12
49	$O + NCO \rightleftharpoons NO + CO$	$2.0 \times 10^{13}$	.0	0.0	12
50	$N + NCO \rightleftharpoons N_2 + CO$	$1.0 \times 10^{13}$		0.0	12
51	$CH + CO_2 \rightleftharpoons HCO + CO$	$3.7 \times 10^{12}$		0.0	12
52	$C_3H_7 \rightleftharpoons C_2H_4 + CH_3$	$4.0 \times 10^{13}$		16 658	12
53	$OH + C_2H_6 \rightleftharpoons H_2O + C_2H_5$	$1.0 \times 10^{14}$		1 761	12
54	$H + C_2H_6 \rightleftharpoons H_2 + C_2H_5$	$1.1 \times 10^{14}$		4 278	12
55	$CH + O_2 \rightleftharpoons HCO + O$	$1.0 \times 10^{13}$		0.0	12
56	$M + C_2H_3 \rightleftharpoons C_2H_2 + H + M$	$3.0 \times 10^{16}$		20 382	12
57	$O + C_2H_2 \rightleftharpoons CH_2 + CO$	$5.2 \times 10^{13}$		1 862	12

<sup>a</sup>Rate constant is given by the equation  $k = AT^n \exp(-\theta/T)$  where T is temperature in K and θ is the ratio of the reaction activation energy to the universal gas constant.

<sup>b</sup>Units of k for a unimolecular reaction are sec<sup>-1</sup>; for a bimolecular reactions units are cm<sup>3</sup>/mole sec and for a termolecular reaction, units are cm<sup>6</sup>/mole<sup>2</sup> sec.

TABLE II. - COMPARISON OF CHEMICAL REACTION AND DILUTION EFFECTS  
FOR MIXTURES WITH 1.0 PERCENT FBN

(a) Dilution to  $\phi_s = 0.7$ .

$\phi_p$	NO <sub>x</sub> concentration, ppm		
	Primary exhaust gas	Diluted primary exhaust gas	Secondary exhaust gas
0.8	2 302	2 019	2056
1.0	3 139	2 242	2291
1.2	1 146	690	801
1.4	627	327	447
CO concentration, ppm			
0.8	4 794	4 205	1415
1.0	19 589	13 992	2409
1.2	57 763	34 797	4579
1.4	96 213	50 111	5983

(b) Dilution to  $\phi_s = 0.5$ .

$\phi_p$	NO <sub>x</sub> concentration, ppm		
	Primary exhaust gas	Diluted primary exhaust gas	Secondary exhaust gas
0.8	2 302	1 466	1472
1.0	3 139	1 618	1628
1.2	1 146	498	505
1.4	627	237	244
CO concentration, ppm			
0.8	4 794	3 054	418
1.0	19 589	10 097	1002
1.2	57 763	25 114	1900
1.4	96 213	36 307	2545

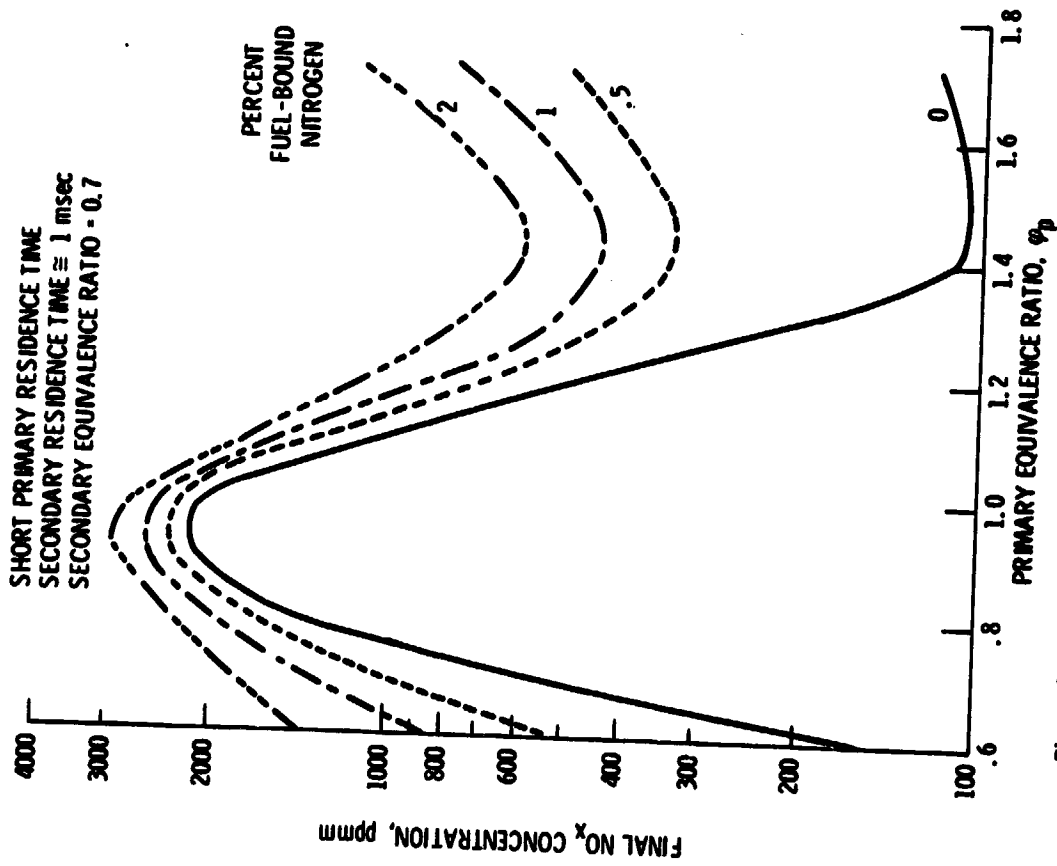


Figure 1. -  $\text{NO}_x$  concentration versus primary equivalence ratio for propane-air.

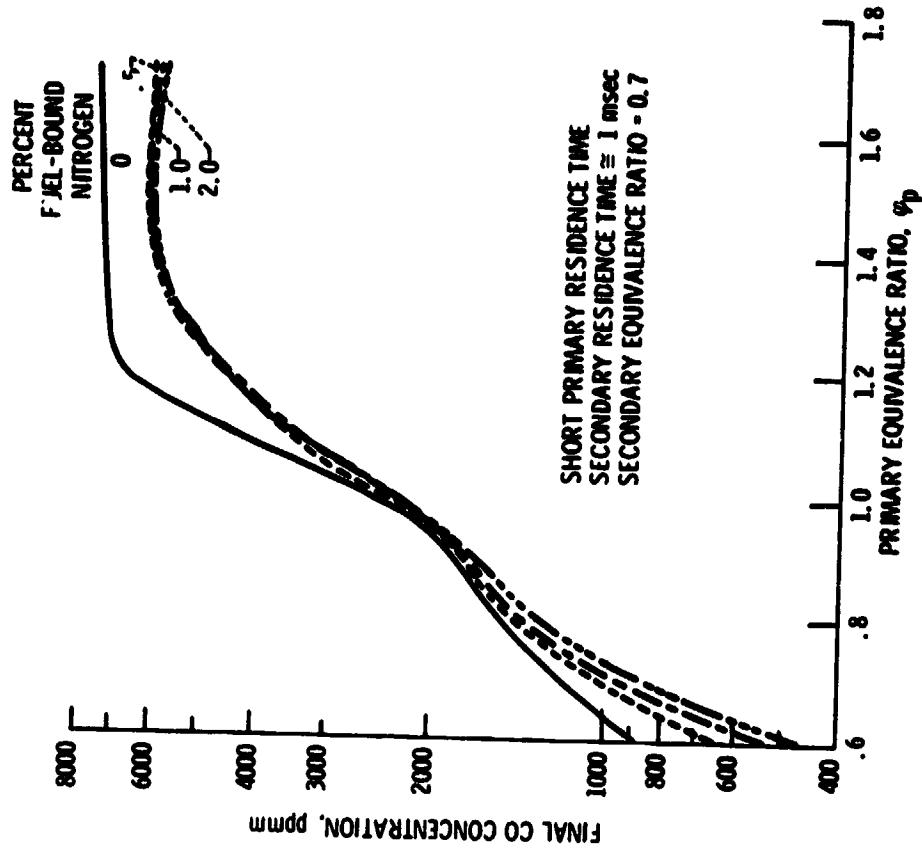


Figure 2. - CO concentration versus primary equivalence ratio.

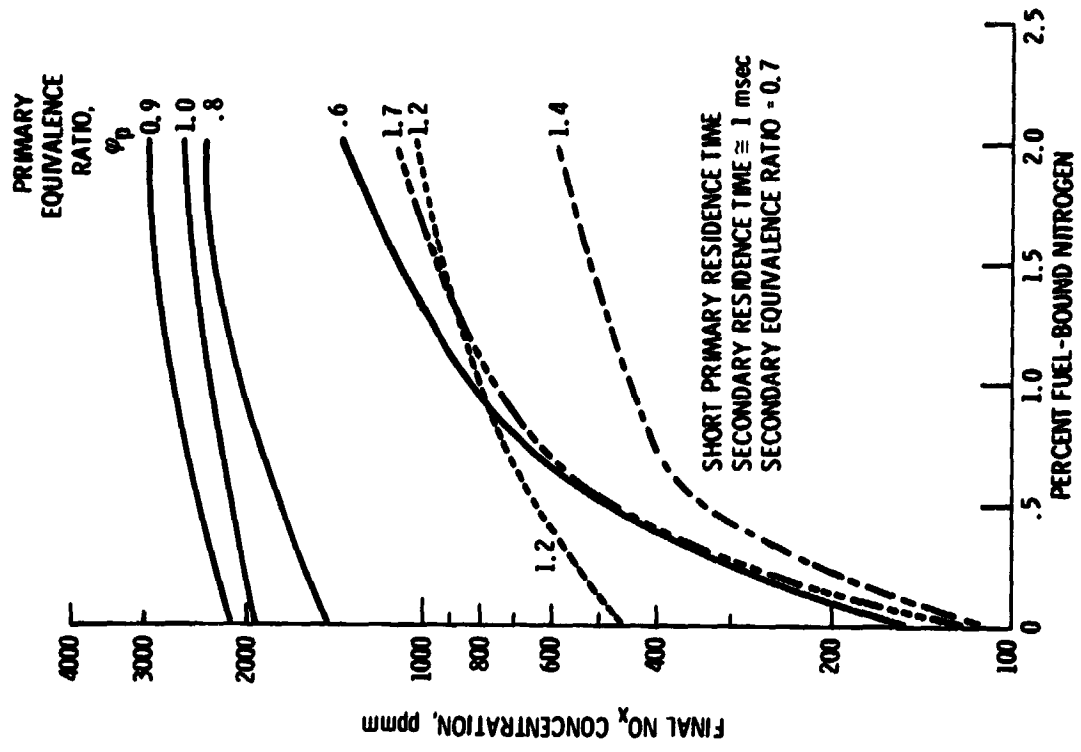


Figure 3. - Effect of fuel-bound nitrogen on final NO<sub>x</sub> concentration.

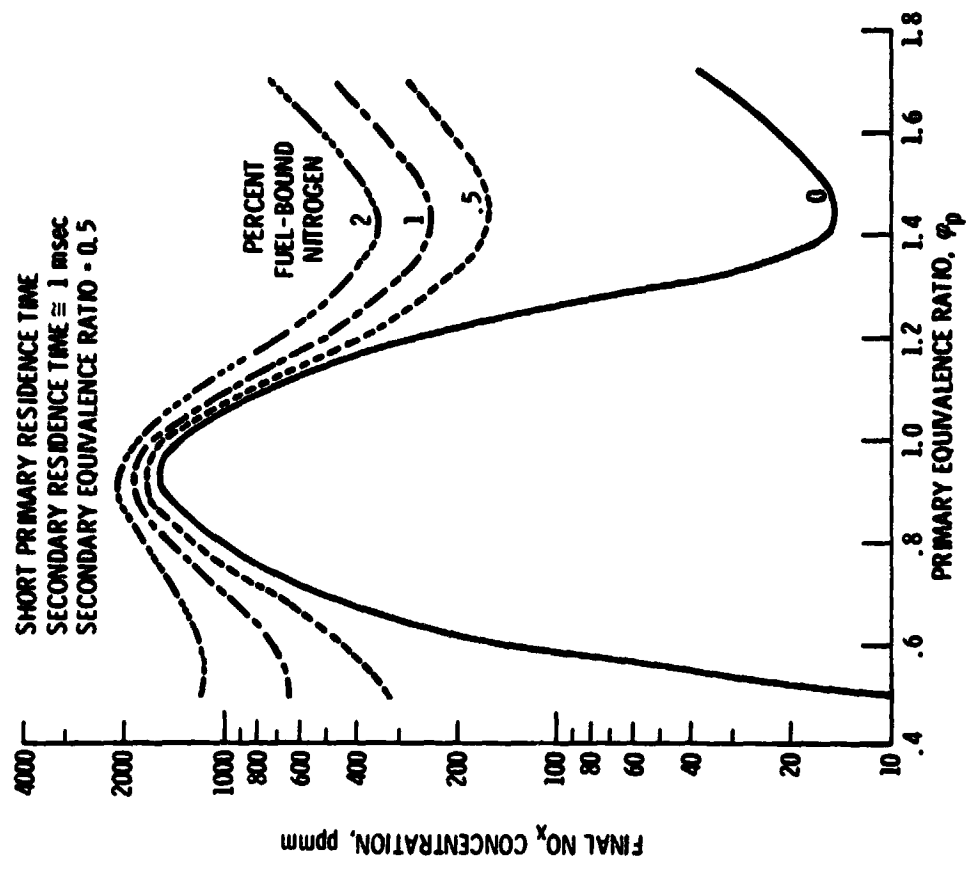


Figure 4. - NO<sub>x</sub> concentration versus primary equivalence ratio for additional secondary dilution.

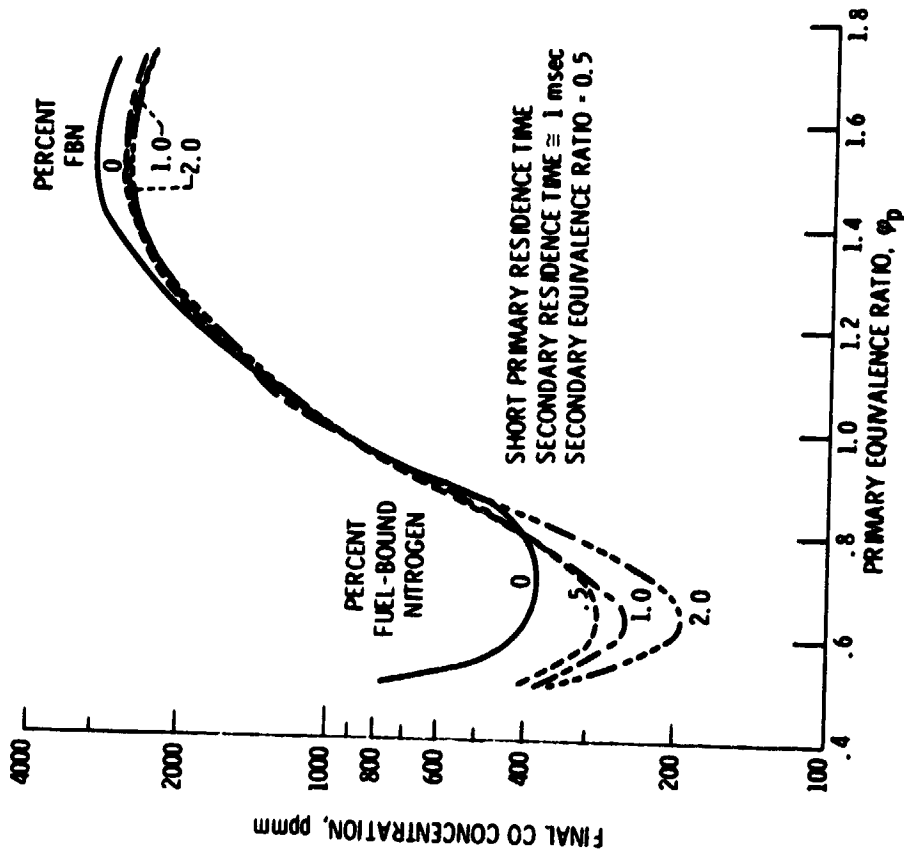


Figure 5. - CO concentration versus primary equivalence ratio for added secondary dilution.

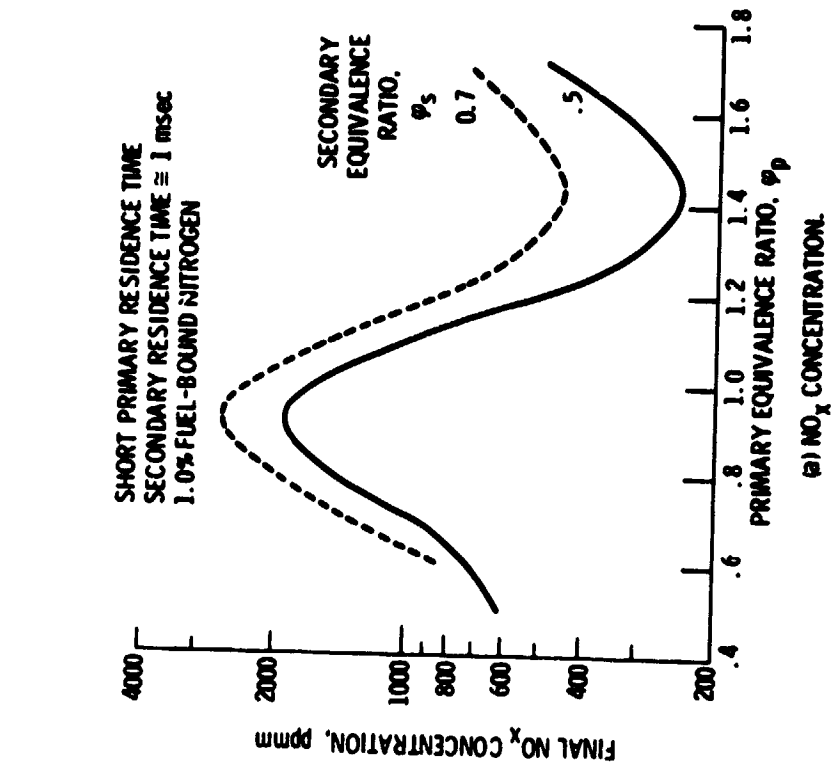


Figure 6. - Effect of secondary dilution.

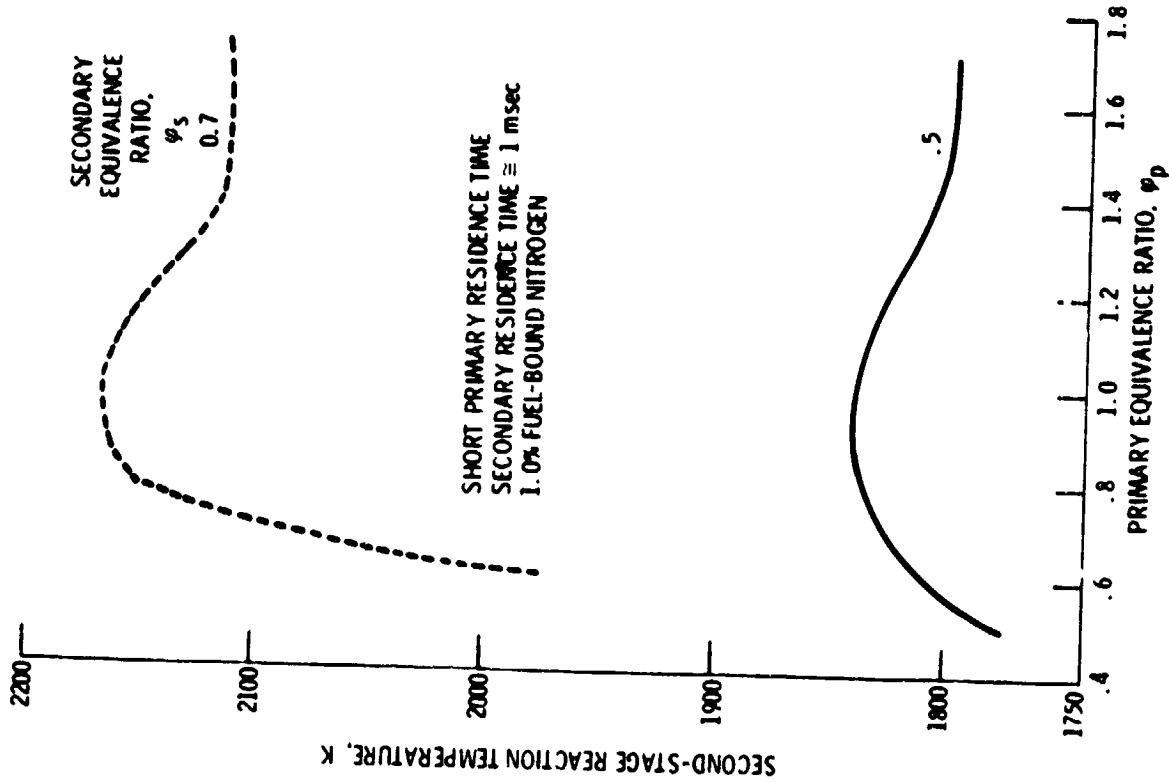


Figure 7. - Effect of secondary dilution on secondary reaction temperature.

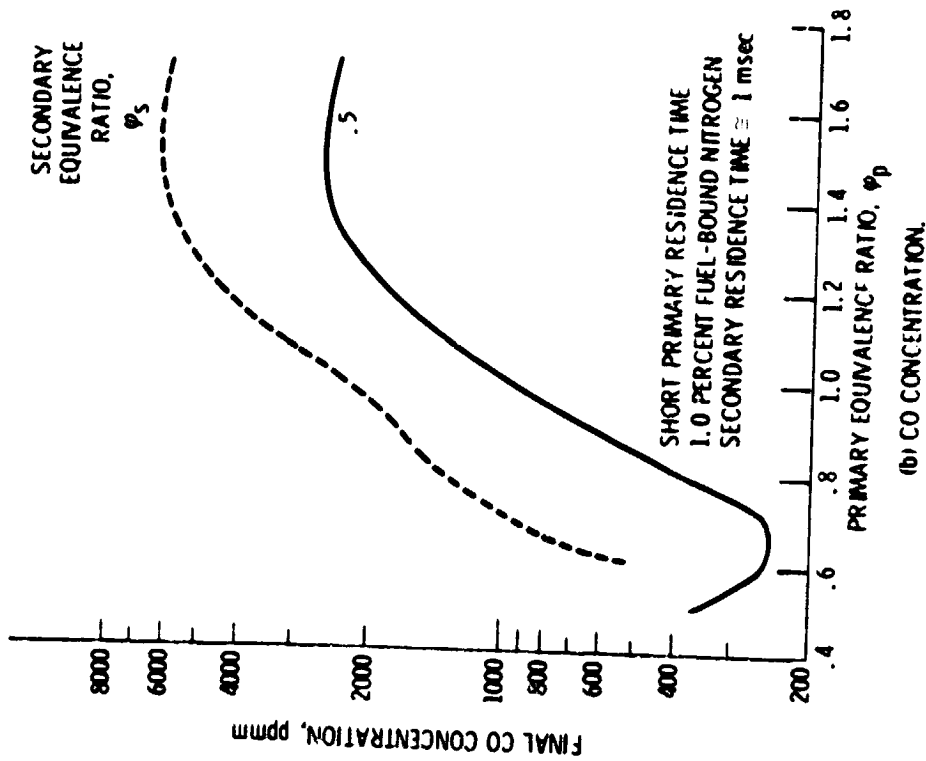


Figure 6. - Effect of secondary dilution.

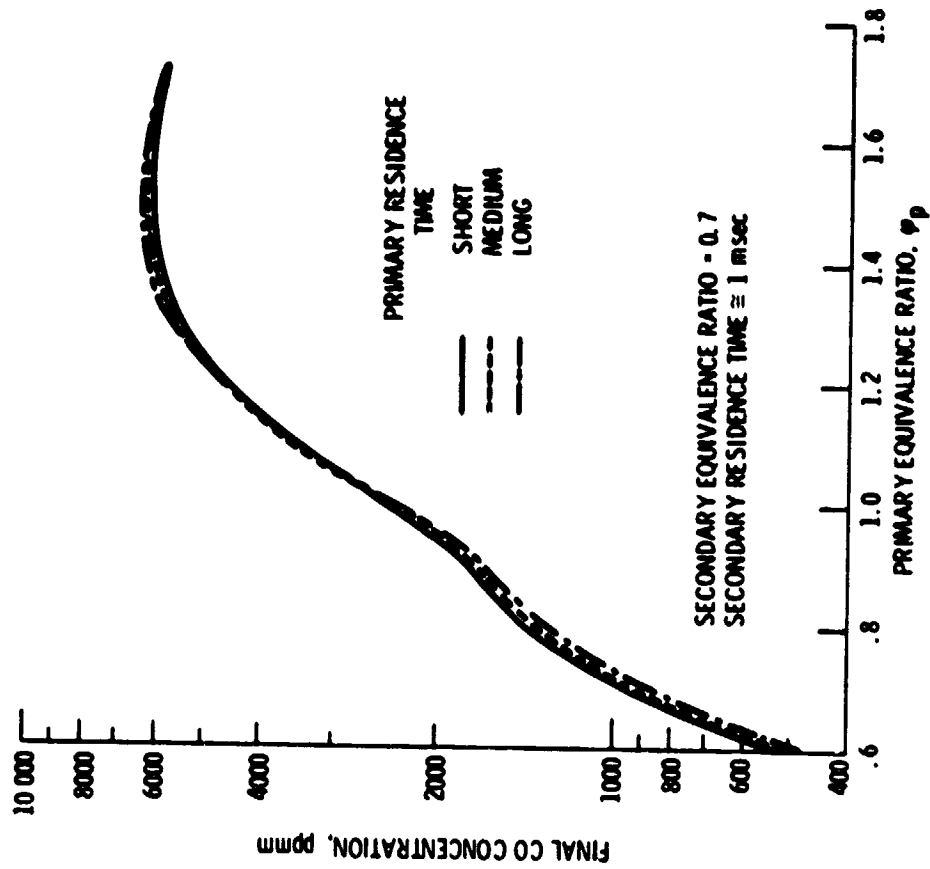


Figure 9. - Effect of primary residence time on CO formation for 1.0 percent fuel bound nitrogen content.

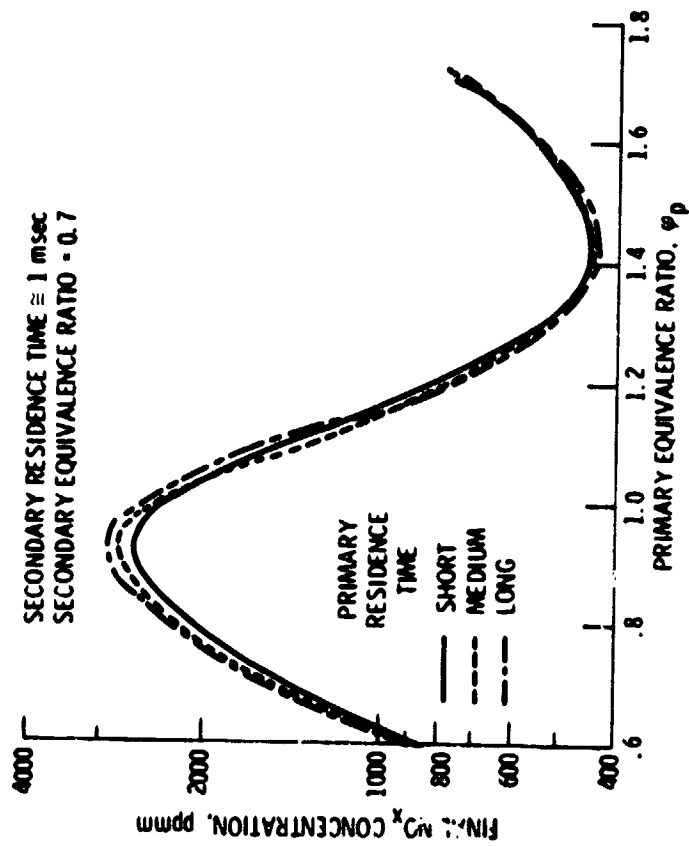
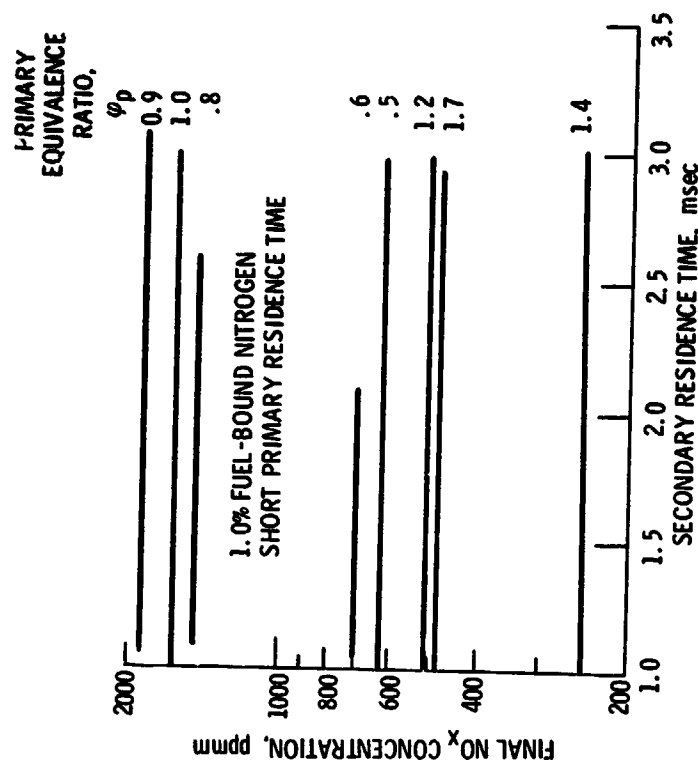
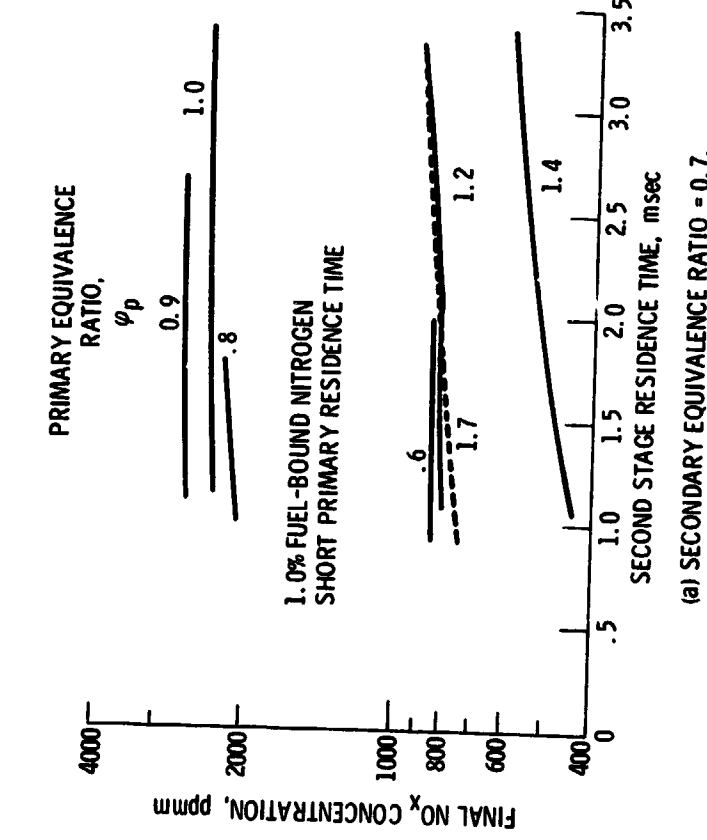


Figure 8. - Effect of primary residence time on  $NO_x$  formation for 1.0 percent fuel-bound nitrogen content.



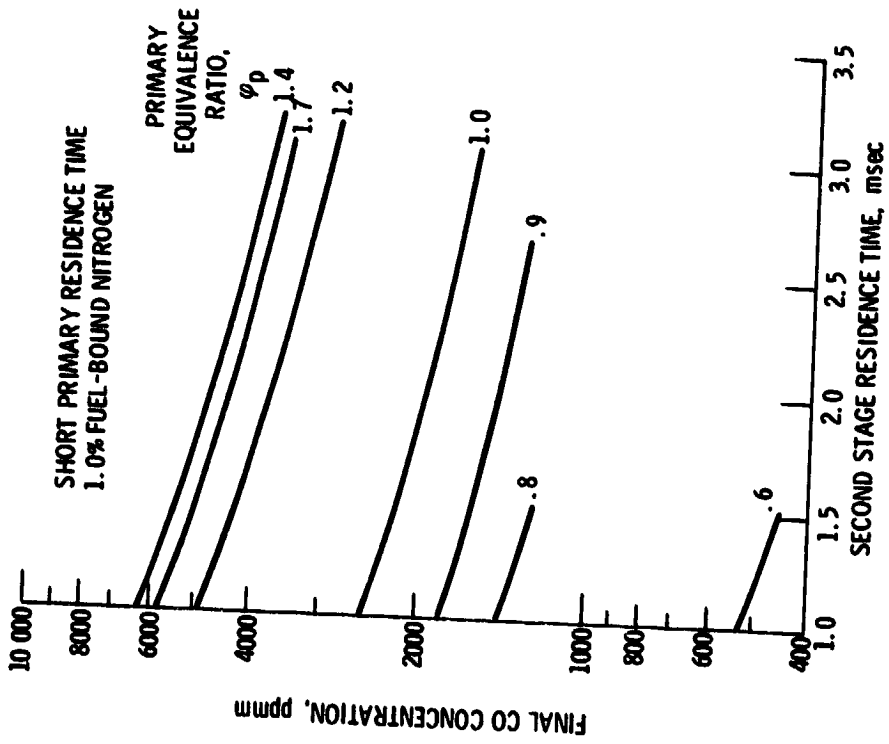
(a) SECONDARY EQUIVALENCE RATIO = 0.7.

Figure 10. - Effect of second stage residence time on final  $\text{NO}_x$  concentration.



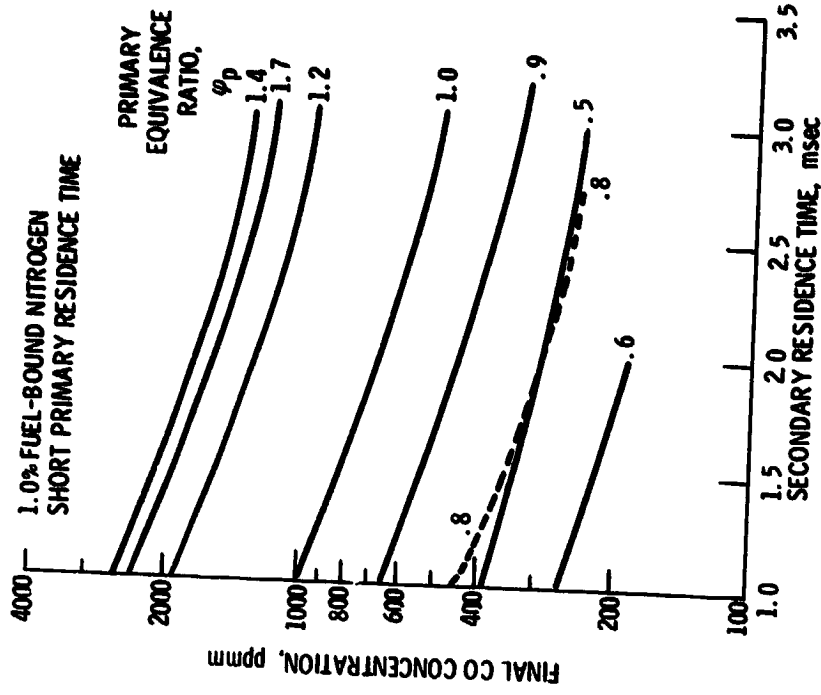
(b) SECONDARY EQUIVALENCE RATIO = 0.5.

Figure 10. - Effect of secondary residence time on final  $\text{NO}_x$  concentration.



(a) SECONDARY EQUIVALENCE RATIO = 0.7.

Figure 11. - Effect of second-stage residence time on final CO concentration.



(b) SECONDARY EQUIVALENCE RATIO = 0.5.

Figure 11. - Effect of secondary residence time on final CO concentration.

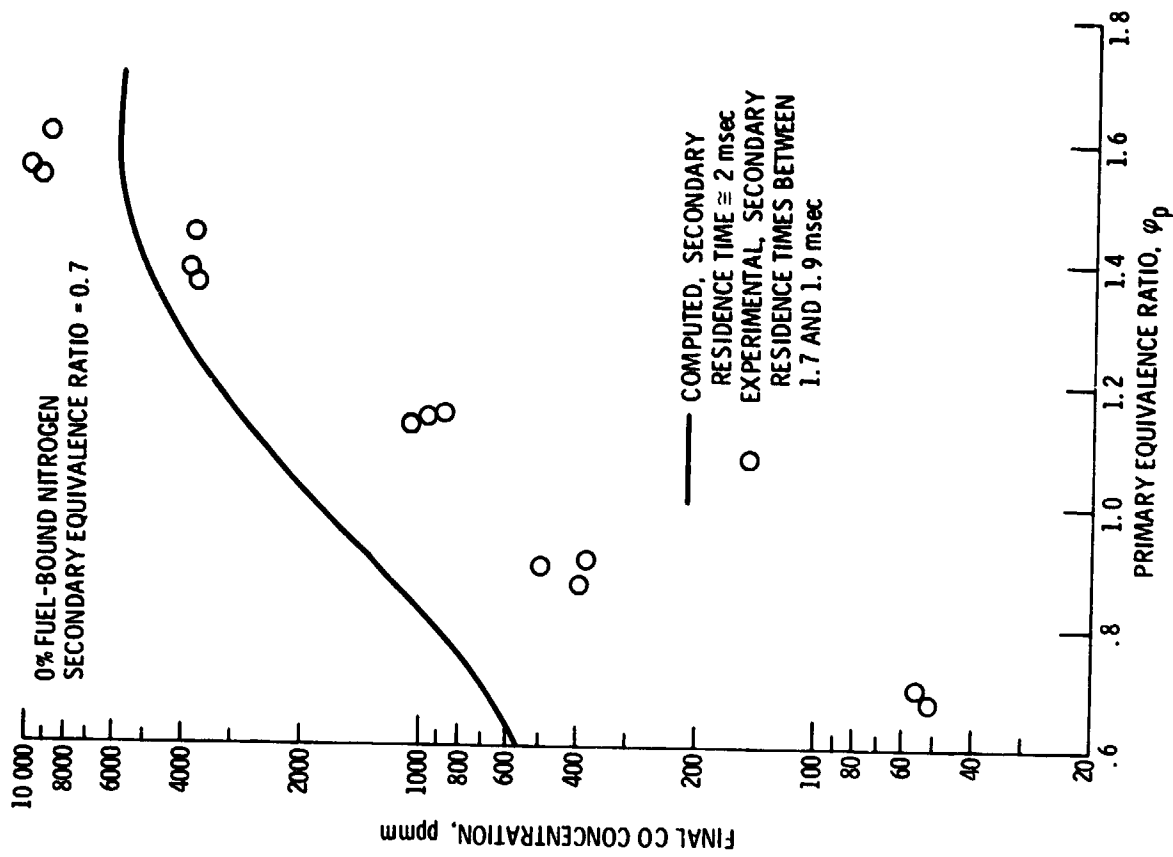


Figure 13. - Comparison of computed and experimental CO concentrations.

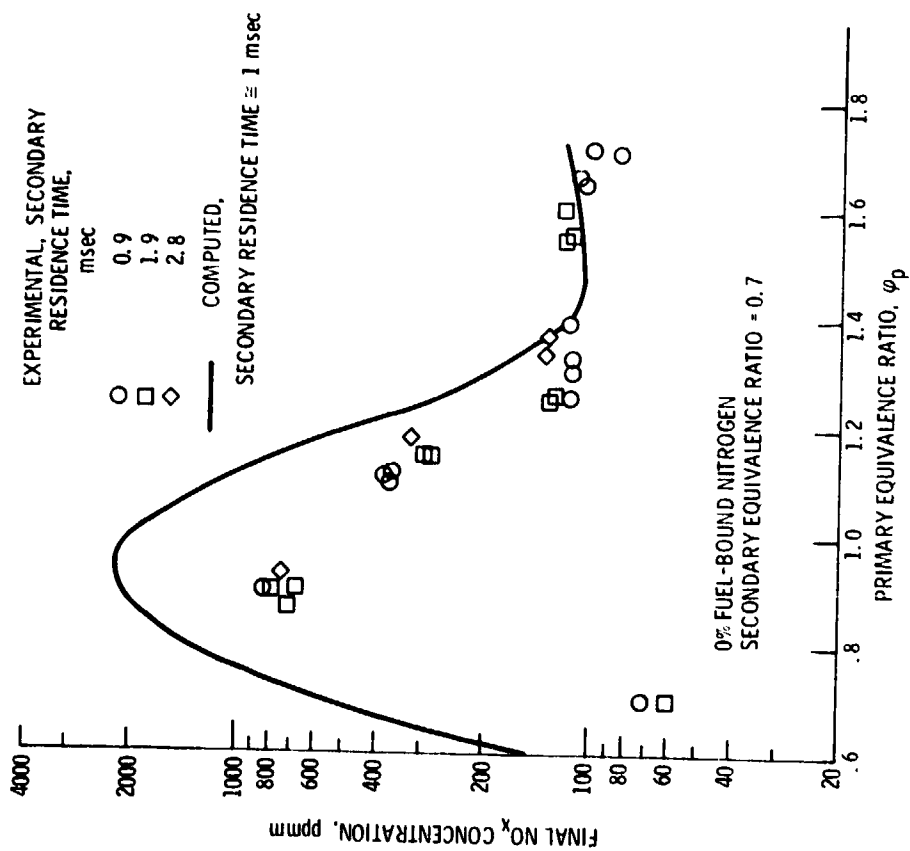


Figure 12. - Comparison of computed and experimental NO<sub>x</sub> concentrations.